Available online at www.sciencedirect.com

ScienceDirect

Procedia Structural Integrity 13 (2018) 1135–1140

Structural Integrity Procedia

www.elsevier.com/locate/procedia

ECF22 - Loading and Environmental effects on Structural Integrity

Reference toughness – a pragmatic tool to estimate ductile-brittle transition temperatures

Sakari Pallaspuro[a,b,*], Saara Mehtonen[c], Jukka Kömi[a], Zhiliang Zhang[b] and David Porter[a]

[a]*Materials and Production Engineering, Centre for Advanced Steels Research, University of Oulu, Finland*
[b]*Department of Structural Engineering, Faculty of Engineering Science and Technology, NTNU, Norway*
[c]*SSAB, Raahe, Finland*

Abstract

Recent advances show that tough as-quenched ultra-high-strength steels in fully and partially martensitic conditions demand proper control of the effective coarse grain size, which is the key microstructural parameter controlling the toughness in the ductile-brittle transition region. The most effective way to reduce this grain size and texture components detrimental to toughness with thermomechanically rolled steels is to apply a high level of austenite pancaking. The effective coarse grain size ($d_{80\%}$) can be used to reliably estimate impact toughness transition temperatures. Adding the fraction of {100} cleavage planes close to the specimen notch/crack plane further improves these estimates. A recent straightforward semi-physical model consists of just two parameters, the first term describes the temperature-dependency of a local brittle fracture, and the second term relates to the size of these locally cleaved areas. Here, we present the concept *reference toughness* and study its applicability to the estimation of both impact toughness and fracture toughness transition temperatures. Fractographic evidence demonstrates that failure initiation is a complicated interaction between large grains and large brittle inclusions. With locally varying, inhomogeneous microstructural properties, the failure is likely to initiate and propagate when a large particle locates in a coarse-grained matrix, whose dimensions are in line with the effective coarse grain size. Application of these microstructure-based estimates of the impact toughness and fracture toughness transition temperatures can further assist the design and production of steels with lath-like microstructures.

Peer-review under responsibility of the ECF22 organizers.

Keywords: Ductile-brittle transition; Stress intensity; Fracture toughness; Impact toughness; Grain size; Characterization

* Corresponding author. Tel.: +358-294-487-481.
E-mail address: sakari.pallaspuro@oulu.fi

2452-3216
Peer-review under responsibility of the ECF22 organizers.
10.1016/j.prostr.2018.12.237

Nomenclature

CFU	cleavage fracture unit size, or cleavage facet size
c_{SR}	coefficient for strain rate dependent yield strength
d_{ecgs}	effective coarse grain size
$d_{80\%}$	effective coarse grain size at 80% of the cumulative probability distribution
f	dimensionless constant for specimen type
K_{ref}	reference toughness
$K_{Id\text{-}ref}$	dynamic reference toughness
T_T	toughness transition temperature
T_0	fracture toughness reference temperature
T_{27J}	27 J Charpy-V impact toughness transition temperature
T_{28J}	28 J Charpy-V impact toughness transition temperature
σ_d	dynamic yield strength
σ_f	fracture stress
σ_{eff}	effective stress
σ_{ys}	room-temperature yield stress

1. Introduction

Knowledge of fracture mechanical behaviour is essential for safe structural design of steel against brittle cleavage fracture. To improve low-temperature toughness, one must identify and strive to eliminate the weakest links in the (micro)structure that can cause the material to fail. In bcc materials, cleavage occurs as a rapid transgranular crack propagation along the crystallographic {100} planes that are the easiest to debond. In order to initiate cleavage fracture, a sharp surface flaw or a local microstructural discontinuity must provide sufficient stress build-up for the bond strength to be exceeded.

Discontinuities that can determine the toughness properties in the transition temperature region divide into three categories: 1) small particles, like carbides and other brittle precipitates (Bowen, Druce, and Knott 1987; Lee et al. 2002), 2) larger inclusions and brittle second phase particles (Echeverría and Rodriguez-Ibabe 1999; Bose Filho, Carvalho, and Bowen 2007), and 3) grains (Barr and Tipper 1947; Wang et al. 2008; Morris, Jr. 2011). Furthermore, the failure initiation can often be a complicated interaction between large grains and large particles (Ghosh et al. 2013).

A simple method to assess the critical flaw size is to assess them with modified Griffith's failure criterion, Eq. (1), where the local cleavage fracture stress σ_f depends on the stress concentration factor c, the modulus of elasticity E, surface energy γ, and the microcrack diameter C_0. In the case of a penny-shaped microcrack ahead of a macroscopic crack tip, which is a feasible approximation for many microstructural features that can be described with an equivalent circle diameter, we have $c = \pi$. Following San Martin and Rodriguez-Ibabe (1999), in the propagation-controlled cleavage cracking temperature range, the surface energy should be the effective surface energy γ_{eff} (often taken as 100 J/m^2). Eq. (1) emphasises the need to minimize the size of the probable weakest links, i.e. the coarsest effective grains (d_{ecgs}).

$$\sigma_f[MPa] = \sqrt{c \times \frac{E\gamma}{(1-\nu^2)C_0}} = \sqrt{\frac{\pi E \gamma_{eff}}{(1-\nu^2)d_{ecgs}}} \quad (1)$$

Of these factors, many studies have been dedicated to relating impact toughness transition temperatures to grain size and other factors (Pickering and Gladman 1963; Mintz, Peterson, and Nassar 1994; Isasti et al. 2014). Recently, Pallaspuro et al. (2018) proposed a semi-physical method to estimate impact toughness transition temperatures (T_{27J}, T_{28J}, and T_{50}) highlighting the importance of the effective coarse grain size d_{ecgs}. That method is based on two factors: 1) a term for the propagation of a local cleavage crack described by a dynamic reference toughness $K_{Id\text{-}ref}$, and 2) a term for the extent of propagation of a continuously cleaved area described with the area fraction of {100} planes oriented within 15° of the macroscopic fracture plane. Supporting that model Pallaspuro (2018) showed with fractographic evidence that, in the case of homogeneous grain size distributions, the cleavage facet size (CFU) at the primary cleavage crack nucleation site corresponded to the 80th percentile of the effective grain size distribution ($d_{80\%}$).

In the case of heterogeneous material, with a bimodal grain size distribution, a better correlation was obtained with the 90th percentile ($d_{90\%}$).

Here in this study, we present the pragmatic concept of reference toughness and extend it to apply to single-edge notched bend specimens (SENB) in addition to Charpy V-notched specimens (CVN) thus covering a range of different notch or crack acuities and strain rates.

2. Reference toughness K_{ref}

In the case of Mode I (opening) loading, the stress intensity K ahead of a crack is given by a specimen geometry dependent dimensionless correction factor Y, the applied stress σ, and the crack length a, Eq. (2). Now, to establish a correlation between critical stress intensity and toughness transition temperatures, we assume that the propagation of a local embedded crack ahead of the macroscopic crack tip is the critical event for failure in the lower half of the ductile-brittle transition temperature region, namely at the energy absorption level around 27 – 28 J in the standardised impact toughness test (ISO 2009) and the stress intensity of around 100 MPa√m in the standardised fracture toughness test (ASTM International 2015). To address both the CVN and SENB specimens, Y×σ needs to be modified to take the differing conditions into account. To address both cracked and notched specimens, Y is replaced with f (Eq. 2), which is the general ratio between σ_f and σ_{ys} for a given specimen type. In the case of SENB specimens, an upper bound for the local fracture stress is $\sigma_f \approx 3.0\times\sigma_{ys}$, matching with the small-scale yielding condition. In the case of CVN specimens, $\sigma_f \approx 2.2\times\sigma_{ys}$, is selected based on the analyses of Green and Hundy (1956) and Griffiths and Owen (1971). This also coincides with the experimental findings for lath-like microstructures (Bose Filho, Carvalho, and Bowen 2007) which gave $\sigma_f/\sigma_{ys} \approx 2.2 \pm 0.2$. In the case of CVN tests, the quasi-static yield stress needs to be increased by a factor c_{SR} to account for the effect of the high strain rate below the notch. The multiplication of σ_{ys} with the above described factors yields the effective stress σ_{eff} of Eq. (3), in which c_{SR} is based on Sedlacek et al. (2008) as shown in Fig. 1 (a). For the higher strength steels considered here, Fig. 1 (b) shows how, in the case of SENB specimens, the effective stress forms an upper limit for fracture stress, as estimated using Eq. (1) together with either $d_{80\%}$ or CFU. This means that, in the case of SENB fracture toughness specimens, it is very likely that there will be a microcrack in the microstructure that is coarse enough to propagate at stress levels equal to or less than σ_{eff}. Finally, the reference toughness can be written as Eq. (4) for an embedded crack, which defines the local stress intensity for the propagation of a local cleavage crack with d_{ecgs}.

$$K_I = Y\sigma\sqrt{\pi a} \tag{2}$$

$$\sigma_{eff} = f c_{SR} \sigma_{ys} \tag{3}$$

$$where\ f = \begin{cases} 3.0, for\ SENB \\ 2.2, for\ CVN \end{cases}\ and\ c_{SR} = \begin{cases} 1.0 \quad , for\ quasi\ static\ loading \\ \sigma_d/\sigma_{ys}\ , for\ \dot{\varepsilon} = 10^3 s^{-1}\ (Fig.\ 1\ a) \end{cases}$$

$$K_{ref.} = \sigma_{eff}\sqrt{\pi d_{ecgs}/2} \tag{4}$$

3. Results and discussion

Eq. (4) is basically the same as dynamic reference toughness $K_{Id\text{-}ref}$ (Pallaspuro et al. 2018) multiplied by f, the addition of which enables its application to different specimen types. Fig. 2. shows the correlation between the toughness transition temperatures T_T and the reference toughness. Fig. 2 (a) comprises data from 50 CVN samples and Fig. 2 (b) from 19 SENB samples with K_{ref} calculated with either $d_{80\%}$ or CFU as the value of d_{ecgs}. For both cases, the fit is satisfactory, and the difference in stress concentration between the specimen types is clear. The slope is somewhat higher for impact toughness (Fig. 2 a) than for fracture toughness specimens (Fig. 2 b). Suitable data for T_0 are still limited, but the trend appears promising. For both cases, strongly bimodal grain size distributions (GSD)(Pallaspuro 2018) yield extremely unconservative estimates. When the calculations are made using CFU for the same samples, they fall inside the standard deviation bands. Thus, in the case of a clearly non-unimodal GSD, grain size measurements may not provide accurate estimates of the transition temperatures.

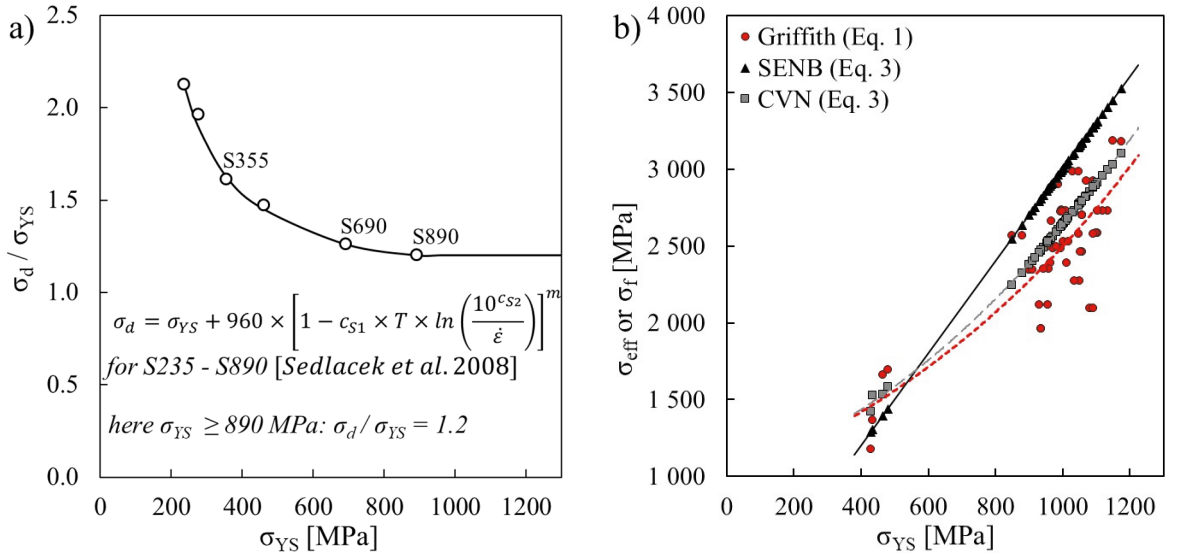

Fig. 1. (a) Elevation of dynamic yield strength, and (b) comparison of the effective stress and cleavage fracture stress in SENB and CVN specimens.

It has been shown that the addition of the fraction of {100} cleavage planes within 15° of the crack plane improves the T_T estimates for CVN specimens and also explaining the effects of specimen orientation on the transition temperatures (Pallaspuro et al. 2018). The addition of the fraction of {100} cleavage planes within 15° of the crack plane also improves the prediction of T_0 by being a rough qualitative measurement that relates to the size of the locally arrested cleavage cracks. With a low {100} fraction, i.e. presumably small continuous {100} planes, it is more likely that an arrested cleavage crack will be too small to cause a significant pop-in (ASTM International 2015) thereby determining the point of failure. However, more data and fractographic investigations are needed to quantify the effect of the actual unit sizes of the {100} cleavage planes within 15° of the crack plane in the case of T_0.

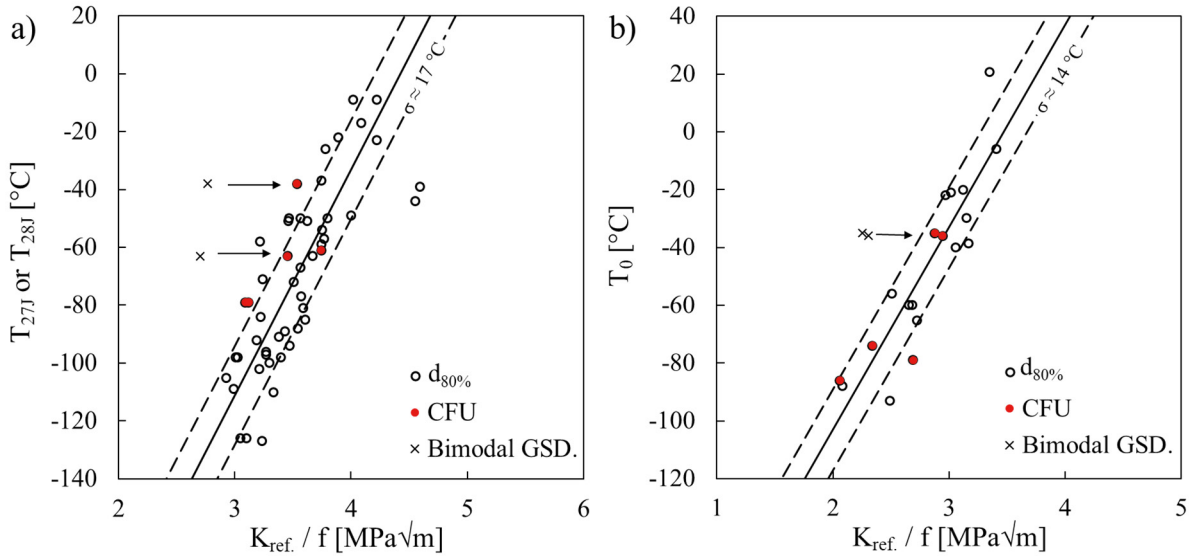

Fig. 2. Toughness transition temperatures (a) T_{27J} and T_{28J}, and (b) T_0 as a function of K_{ref} / f. Samples with a bimodal grain size distribution fall into the trend when CFU is used instead of $d_{80\%}$.

Finally, Fig. 3 shows how K_{ref} describes both the impact toughness transition temperature and fracture toughness reference temperature with a root mean square error of 18 °C. The 95 % confidence limit shows the uncertainty in the slope, and the 95 % prediction limit the overall goodness of the estimate. Fig 3. covers a yield strength range of 430…1175 MPa, 8 tempered and 61 as-quenched samples with a range of fully and partially martensitic microstructures, and a few fully bainitic samples. However, low-strength ferritic-pearlitic steels and steels with mixed non-lath-like microstructures showed significant scatter and are not included here. Those demand still further investigation. Also, while a linear fit can describe the studied population, the actual shape of the curve for a wider range of steels remains open.

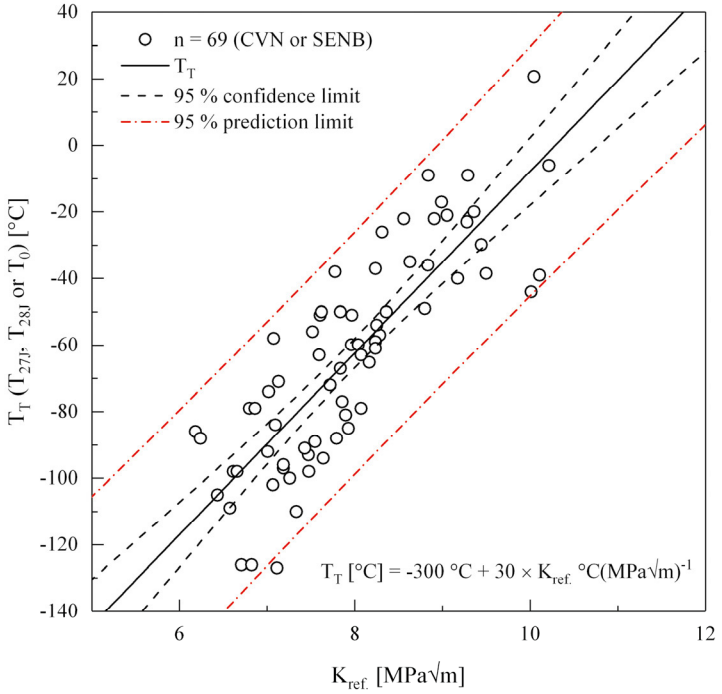

Fig. 3. Ductile-brittle transition temperatures of impact toughness and fracture toughness as a function of reference toughness K_{ref}.

4. Summary

The presented concept of reference toughness is based on the finding that the coarsest grains or brittle particles of a similar size in the microstructure control the overall toughness in the transition temperature range where the fracture process is propagation-controlled. The reference toughness is a pragmatic microstructure-based parameter that can be used as a first estimate for both the impact toughness transition temperatures and the fracture toughness reference temperature. More work is still needed to verify the assumptions presented.

Acknowledgements

Funding from the Academy of Finland to the project Genome of Steel is gratefully acknowledged.

References

ASTM International. 2015. *E1921-14a: Standard Test Method for Determination of Reference Temperature, T0, for Ferritic Steels in the Transition Range*. *ASTM Book of Standards*. doi:10.1520/E1921-05.

Barr, W, and CF Tipper. 1947. “Brittle Fracture in Mild-Steel Plates.” *Journal of the Iron & Steel Institute* 157 (2): 223.

Bose Filho, W. W., A. L M Carvalho, and P. Bowen. 2007. “Micromechanisms of Cleavage Fracture Initiation from Inclusions in Ferritic Welds. Part I. Quantification of Local Fracture Behaviour Observed in Notched Testpieces.” *Materials Science and Engineering A* 460–461:

436–52. doi:10.1016/j.msea.2007.01.115.
Bowen, P., S. G. Druce, and J. F. Knott. 1987. “Micromechanical Modelling of Fracture Toughness.” *Acta Metallurgica* 35 (7): 1735–46. doi:10.1016/0001-6160(87)90119-2.
Echeverría, A., and J. M. Rodriguez-Ibabe. 1999. “Brittle Fracture Micromechanisms in Bainitic and Martensitic Microstructures in a C-Mn-B Steel.” *Scripta Materialia* 41 (2): 131–36. doi:10.1016/S1359-6462(99)00124-4.
Ghosh, A., A. Ray, D. Chakrabarti, and C. L. Davis. 2013. “Cleavage Initiation in Steel: Competition between Large Grains and Large Particles.” *Materials Science and Engineering A* 561. Elsevier: 126–35. doi:10.1016/j.msea.2012.11.019.
Green, A P, and B B Hundy. 1956. “Initial Plastic Yielding in Notch Bend Tests.” *Journal of the Mechanics and Physics of Solids* 4: 128–44.
Griffiths, J R, and D R J Owen. 1971. “An Elastic-Plastic Stress Analysis for a Notched Bar in Plane Strain Bending.” *Journal of Mechanics and Physics of Solids* 19: 419–31.
Isasti, Nerea, Denis Jorge-Badiola, Mitra L. Taheri, and Pello Uranga. 2014. “Microstructural Features Controlling Mechanical Properties in Nb-Mo Microalloyed Steels. Part II: Impact Toughness.” *Metallurgical and Materials Transactions A* 45 (11). Springer US: 4972–82. doi:10.1007/s11661-014-2451-6.
ISO. 2009. *EN ISO 148-1: Metallic Materials, Charpy Pendulum Impact Test, Part 1: Test Method*.
Lee, S, S Kim, B Hwang, B S Lee, and C G Lee. 2002. “Effect of Carbide Distribution on the Fracture Toughness in the Transition Temperature Region of an SA 508 Steel.” *Acta Materialia* 50 (19): 4755–62. doi:10.1016/S1359-6454(02)00313-0.
Mintz, B, G Peterson, and A Nassar. 1994. “Structure-Property Relationships in Ferrite-Pearlite Steels.” *Ironmaking & Steelmaking* 21 (3). Maney: 215–22.
Morris, Jr., John William. 2011. “On the Ductile-Brittle Transition in Lath Martensitic Steel.” *ISIJ International* 51 (10): 1569–75. doi:10.2355/isijinternational.51.1569.
Pallaspuro, Sakari. 2018. *On the Factors Affecting the Ductile-Brittle Transition in as-Quenched Fully and Partially Martensitic Low-Carbon Steels*. Acta Unive. Oulu: University of Oulu.
Pallaspuro, Sakari, Antti Kaijalainen, Saara Mehtonen, Jukka Kömi, Zhiliang Zhang, and David Porter. 2018. “Effect of Microstructure on the Impact Toughness Transition Temperature of Direct-Quenched Steels.” *Materials Science & Engineering A* 712: 671–80. doi:10.1016/j.msea.2017.12.037.
Pickering, F B, and T Gladman. 1963. “Metallurgical Developments in Carbon Steels.” *Iron and Steel Institute Special Report* 81: 10–25.
San Martin, J I, and J M Rodriguez-Ibabe. 1999. “Determination of Energetic Parameters Controlling Cleavage Fracture in a Ti-V Microalloyed Ferrite-Pearlite Steel.” *Scripta Materialia* 40 (4): 459–64. doi:10.1016/S1359-6462(98)00467-9.
Sedlacek, G, M Feldmann, B Kühn, D Tschickardt, S Höhler, C Müller, W Hensen, et al. 2008. “Commentary and Worked Examples to EN 1993-1-10 “Material Toughness and through Thickness Properties" and Other Toughness Oriented Rules in EN 1993.”
Wang, Chunfang, Maoqiu Wang, Jie Shi, Weijun Hui, and Han Dong. 2008. “Effect of Microstructural Refinement on the Toughness of Low Carbon Martensitic Steel.” *Scripta Materialia* 58 (6): 492–95. doi:10.1016/j.scriptamat.2007.10.053.